Transition between Tonic Spiking and Bursting in a Neuron Model via the Blue-Sky Catastrophe

Andrey Shilnikov[1] and Gennady Cymbalyuk[2,*]
[1]Department of Mathematics and Statistics, Georgia State University, Atlanta, Georgia 30303, USA
[2]Department of Physics and Astronomy, Georgia State University, Atlanta, Georgia 30303, USA

(Received 7 June 2004; published 31 January 2005)

We study a continuous and reversible transition between periodic tonic spiking and bursting activities in a neuron model. It is described as the blue-sky catastrophe, which is a homoclinic bifurcation of a saddle-node periodic orbit of codimension one. This transition constitutes a biophysically plausible mechanism for the regulation of burst duration that increases with no bound like $1/\sqrt{\alpha - \alpha_0}$ as the transition value α_0 is approached.

DOI: 10.1103/PhysRevLett.94.048101 PACS numbers: 87.19.La, 05.45.–a, 87.17.Nn, 87.19.Nn

The bursting activity of neurons has been described in terms of the qualitative theory of slow-fast systems [1–4]. The classification of routes describing possible transitions between tonic spiking and bursting is yet incomplete and remains a fundamental problem for both neuroscience and the theory of dynamical systems [5–9]. Qualitative description of a transition yields quantitative information about changes of physical characteristics associated with the transition. This approach has proven exemplary in neuroscience for studies of transitions between silence and tonic spiking. It identifies dependence of the spiking frequency and amplitude on control parameters [10,11] and predicts cooperative behavior of weakly coupled neurons [10,12]. Similarly, applications of the qualitative theory of slow-fast systems to the identification of transitions between tonic spiking and bursting can provide vital information about the neuronal dynamics.

One of the routes from tonic spiking into bursting is distinguished by the following events as a control parameter is varied; the periodic spiking undergoes a series of period-doubling bifurcations followed by a homoclinic bifurcation of a saddle equilibrium [5,6,13,14]. Terman [5] gives a rigorous proof of the existence of Smale horseshoes in this case, so chaos is a key signature for transitions of this kind.

In [15] we described a different transition mechanism based on a saddle-node bifurcation for periodic orbits with noncentral homoclinics [16]. At this bifurcation, a stable periodic orbit representing tonic spiking merges with a saddle periodic orbit having transverse homoclinic trajectories. It is distinguished by a bistability in the system such that either tonic spiking or bursting (periodic and chaotic) can be observed. As a control parameter α decreases to the transition value α_0, the burst duration can be as long as $|\ln(\alpha - \alpha_0)|$. Realization of this mechanism predicts that there exist critical control parameter values for which the system can generate a train of bursts before it finally settles down into periodic spiking. This intermittency is a consequence of Smale horseshoe dynamics.

Here, we suggest a novel mechanism describing a reversible and continuous transition between spiking and bursting in neuron models. It is based on a codimension-one bifurcation known as the blue-sky catastrophe [17–19]. Our study is the first application of this novel bifurcation to realistic neuron models and to any physical system in general. Rigorous proofs and three scenarios of the blue-sky catastrophe in singularly perturbed systems can be found in [20]. In [18] this bifurcation was shown to occur in a modified Hindmarsh-Rose model. The geometry of the bifurcation is illustrated in Fig. 1(a). At the bifurcation, there exists a saddle-node periodic orbit whose two-dimensional unstable manifold W^u returns to the periodic orbit making infinitely many rotations in the node (attracting) region. As a control parameter passes the critical value, the saddle-node periodic orbit disappears and a long stable periodic orbit is born [Fig. 1(b)]. The infinite period of the periodic bursting is due to the slow passage of the phase point through the "phantom" of the disappeared saddle-node periodic orbit.

We study this transition in a model of a heart interneuron from the medicinal leech. It describes well the dynamics of the neuron under normal and pharmacologically modified conditions [21–23]. Under pharmacological conditions, which block Ca^{2+} currents and the hyperpolarization activated inward current and partially block outward currents [24], the neuron can be described by the model based on just two currents, noninactivating K^+ current, I_{K2}, and transient Na^+ current, I_{Na} [21]. It is described by

$$\begin{aligned} CV' &= -[\bar{g}_{K2} m_{K2}^2 (V - E_K) + g_l (V - E_l) \\ &\quad + \bar{g}_{Na} h_{Na} (V - E_{Na}) f(-150, 0.0305, V)^3 + I_{pol}], \\ m'_{K2} &= [f(-83, 0.018 + V_{K2}^s, V) - m_{K2}]/\tau_{K2}, \\ h'_{Na} &= [f(500, 0.0325, V) - h_{Na}]/\tau_{Na}, \end{aligned} \tag{1}$$

where the variables V, m_{K2}, and h_{Na} are the membrane potential, activation of I_{K2}, and inactivation of I_{Na}, respectively; I_{pol} is a polarizing current; $\bar{g}_{K2}$ and $\bar{g}_{Na}$ are the maximum conductances of I_{K2} and I_{Na}, correspondingly; E_K and E_{Na} are the reversal potentials of K^+ and Na^+, respectively; g_l and E_l are the conductance and reversal potential of the leak current, respectively; $C = 0.5$ nF is the membrane capacitance; V_{K2}^s is a parameter shifting the

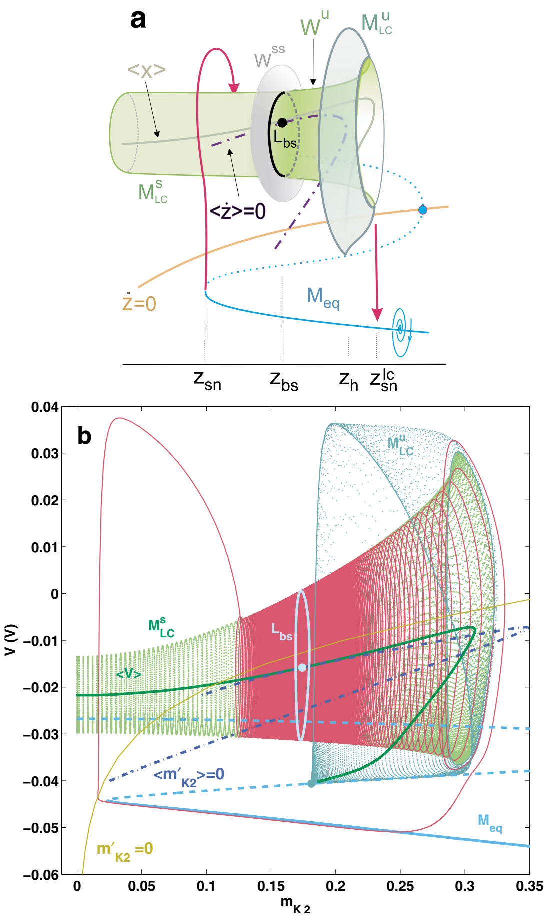

FIG. 1 (color). Phenomenological sketch (a) and matching numerical portrait (b) of the model (1) at the blue-sky catastrophe. A saddle-node periodic orbit $L_{\rm bs}$ is depicted in (a) for the slow-fast system (2) in the (z, x) phase space combined with the bifurcation diagram of its fast subsystem, in (b) for the neuron system (1) in $(m_{\rm K2}, V)$ phase space for $V^s_{\rm K2} = 24.5$ mV. The blue Z-shaped line, $M_{\rm eq}$, consists of the equilibrium states of the fast subsystem (dotted and solid segments represent unstable and stable ones). The point of its intersection with the regular nullcline $\dot{z} = 0$ in (a) and $m'_{\rm K2} = 0$ in (b) is an equilibrium state of the system. The green cylinder-shaped surface $M_{\rm LC} = M^s_{\rm LC} \cup M^u_{\rm LC}$ is composed of the stable and unstable limit cycles of the fast subsystem. The line $\langle x\rangle$ shows the dependence of the x coordinate of the limit cycle averaged over its period on z, and $\langle V\rangle$ vs $m_{\rm K2}$ in (b). The dashed, blue line is the average nullcline $\langle\dot{z}\rangle = 0$ in (a) and $\langle m'_{\rm K2}\rangle = 0$ in (b). The contact point between $\langle V\rangle$ and $\langle m'_{\rm K2}\rangle = 0$ corresponds to the saddle-node periodic orbit, $L_{\rm bs}$. The gray disk W^{ss} in (a) is its strongly stable manifold. The part of $M^s_{\rm LC}$ to the right of $L_{\rm bs}$ is the unstable manifold, W^u of the saddle-node periodic orbit. In (a), the red line outlines rapid transitions of the phase point between the hyperpolarized phase and tonic spiking phase of bursting. In (b), the red curve represents a trajectory homoclinic to $L_{\rm bs}$. This trajectory transforms into a closed periodic orbit representing bursting as parameter $V^s_{\rm K2}$ passes a bifurcation value and $L_{\rm bs}$ disappears.

activation curve of $I_{\rm K2}$; $\tau_{\rm K2}$ and $\tau_{\rm Na}$ are the time constants of activation of $I_{\rm K2}$ and inactivation of $I_{\rm Na}$, respectively; the function f is given by $f(a, b, V) = 1/(1 + e^{a(V+b)})$. The values of the parameters used in this study are $I_{\rm pol} = 0.006$ nA, $\bar{g}_{\rm K2} = 30$ nS, $E_{\rm K} = -0.07$ V, $E_{\rm Na} = 0.045$ V, $\bar{g}_{\rm Na} = 160$ nS, $g_l = 8$ nS, $E_l = -0.046$, $\tau_{h_{\rm K2}} = 0.9$ s, and $\tau_{h_{\rm Na}} = 0.0405$ s. We use $V^s_{\rm K2}$ as a control parameter. In the model, $\tau_{\rm K2}$ is about 20 times larger than $\tau_{\rm Na}$ and the time constant of V and the inactivation of $I_{\rm Na}$. Hence, $m_{\rm K2}$ is the slow variable and the two other variables are the fast ones, so the model (1) can be viewed as a slow-fast system:

$$\dot{\mathbf{x}} = F(\mathbf{x}, z), \qquad \dot{z} = \mu G(\mathbf{x}, z, \alpha) \equiv \mu(g(\mathbf{x}, \alpha) - z), \quad (2)$$

where $\mathbf{x} \in R^n$, $n \geq 2$, and $z \in R^1$; α is a control parameter and $\mu \equiv 1/\tau \ll 1$. The last condition indicates that the dynamics in z is slow in time. We also assume that the functions are smooth enough; furthermore, G is linear in z such as the function on the right-hand side of the slow, middle subsystem in (1), in particular, and in a generic neuron model following Hodgkin-Huxley formalism [25]. At $\mu = 0$, the fast subsystem becomes independent of the slow one. The z variable can then be treated as a bifurcation parameter in the fast subsystem. We call the $(z, \mathbf{x})$ space the extended phase space of the fast subsystem. We suppose that as z increases the fast subsystem undergoes a number of bifurcations illustrated by Fig. 1(a).

Stationary states in the fast subsystem are determined by condition $F(\mathbf{x}, z) = 0$. It yields an equation $x = x_{\rm eq}(z)$ for a spatial curve $M_{\rm eq}$ in the extended $(z, \mathbf{x})$-phase space. As in most models of neurons, the curve $M_{\rm eq}$ has the Z shape (see Fig. 1). In our case, its upper and middle branches consist of repelling and saddle equilibria, whereas the lower branch is composed of stable equilibria of the fast subsystem. The left knee point corresponds to a saddle-node bifurcation where two equilibrium states, one stable and one of the saddle type, merge and vanish for $z < z_{\rm sn}$. We suppose also that when $z < z_{\rm sn}$ the fast subsystem possesses an exponentially stable limit cycle. As z increases, the stable limit cycle traces out a cylindrical-like surface, $M^s_{\rm LC}$, in the extended $(z, \mathbf{x})$ space, which terminates at $z = z^{lc}_{\rm sn}$ where it merges with the surface $M^u_{\rm LC}$ spanned by the unstable limit cycles. Together, $M^s_{\rm LC} \cup M^u_{\rm LC}$ defines the surface $M_{\rm LC}$ of the periodic solutions $x_{lc} = \varphi(t; z)$. Its unstable constituent, M^u_{lc}, adjoins to the curve $M_{\rm eq}$ at some $z = z_h$ [Fig. 1(a)]. Here, the unstable limit cycle becomes a homoclinic loop of a saddle equilibrium state on the middle branch of $M_{\rm eq}$. An average value $\langle x\rangle$ on the limit cycle $\varphi(t; z)$ over its period T for each z is given by $\langle x\rangle = \frac{1}{T(z)} \int_0^{T(z)} \varphi(t; z)dt$. The graph of $\langle x\rangle$ versus z has a knee point at $z = z^{lc}_{sn}$ in the extended (z, x) phase space. This curve terminates at the saddle equilibrium on $M_{\rm eq}$ at $z = z_h$. The knee point corresponds to the saddle-node bifurcation of the limit cycles in the fast subsystem which merge and vanish for $z > z^{lc}_{\rm sn}$.

Let us discuss the dynamics of the system (2) for $0 < \mu \ll 1$ with z being a slow variable. The surface where $\dot{z} = 0$, such that $\dot{z} < 0$ ($\dot{z} > 0$) below (above) it, is called a nullcline. For the system to exhibit oscillations, the nullcline is to cross the unstable branch of the curve M_{eq}, as in Fig. 1(b); this condition guarantees that the whole system has no stable equilibrium state. The slow equation $\dot{z} = \mu G(x_{\mathrm{eq}}(z), z, \alpha)$ gives the first order approximation for the z component of the phase point moving along M_{eq}, with the rate $\sim\mu \ll 1$. Observe that along the hyperpolarized (stable) branch the phase point slowly moves leftward until its z coordinate reaches z_{sn} and the phase point makes a fast switch onto the cylindrical surface M_{LC}. On average, the winding motion of the phase point around M_{LC} is described by its slow translation along the curve $\langle x\rangle$. The dynamics of the z variable around M_{LC} is governed, in first approximation, by the equation $\dot{z} = \mu\langle G(z, \alpha)\rangle \equiv \mu/T(z)\int_0^{T(z)} G(\varphi(t; z); z, \alpha)dt$. When $\dot{z} > 0$ ($\dot{z} < 0$) on the curve $\langle x\rangle$, the phase point moves rightward (leftward) along the cylindrical surface M_{LC}. Having $\dot{z} > 0$, the phase point makes winding motions around the cylinder slowly translating towards the edge of M_{LC} where it switches back onto M_{eq} to start a new cycle of bursting.

Let the function $\langle G\rangle$ have a pair of zeros on the interval $[z^1_{\mathrm{sn}}; z^{lc}_{\mathrm{sn}}]$ at some $z^0_i(\alpha)$, $i = 1, 2$. It follows from Pontryagin-Rodygin's theory [26] that each zero corresponds to a periodic orbit of the whole, singularly perturbed system. Stability of a robust periodic orbit is determined by two factors. First, its stability in the x space follows from the stability of the corresponding robust limit cycle in the phase space of the fast subsystem for the given $z^0_i(\alpha)$. Second, it is stable in z if $\partial\langle G\rangle/\partial z < 0$ at $z^0_i(\alpha)$, and unstable otherwise.

Let the distance between the zeros be controlled by α so that it vanishes at some $\alpha = \alpha_0$. Then, a plain saddle-node bifurcation occurs at α_0 provided that $\partial^2\langle G\rangle/\partial z^2 \neq 0$ at the critical point, and hence the distance between the points is evaluated as $\sim\sqrt{\alpha - \alpha_0}$. Introduce next an averaged nullcline $\langle\dot{z}\rangle = 0$ as the graph defined by the points $(\langle g\rangle; \langle x\rangle)$, where $\langle g(z, \alpha)\rangle = 1/T(z)\int_0^{T(z)} g(\varphi(t; z), \alpha)dt$; note that both components depend parametrically on z. If for given α this nullcline $\langle\dot{z}\rangle = 0$ crosses transversally the curve $\langle x\rangle$, then the z coordinate of such an intersection point is evidently a simple zero of the function $\langle G(z)\rangle$, i.e., equals z^0_i. Recall that $\langle G(z^0_i)\rangle = 0$ means $\langle g(z, \alpha)\rangle - z^0_i = 0$ as follows from (2). This observation lets one visualize effectively the locations of the periodic orbits in the phase space of the singularly perturbed system, as well as determine their possible bifurcations. The approach is used for the model (1) to create a partition of its phase space shown in Fig. 1(b), with $\langle V\rangle$ and $\langle m^l_{\mathrm{K2}}\rangle = 0$ standing for the corresponding nullclines.

Variations of α translate the curve $\langle\dot{z}\rangle = 0$ in the $(z, \mathbf{x})$ space, so that one may make both curves have a quadratic tangency for some $\alpha = \alpha_0$. This saddle-node bifurcation for the periodic orbits constitutes the first component of the blue-sky catastrophe in slow-fast systems. A plain saddle-node periodic orbit in R^n, $n \geq 3$, has two unique manifolds. The strongly stable manifold W^{ss} divides locally a vicinity of the saddle-node orbit into two regions: node and saddle [see Fig. 1(a)]. In the node region, a trajectory is attracted to the periodic orbit. In the saddle region, the periodic orbit is repelling. The unstable manifold W^u consists of the trajectories which are attracted to the saddle-node periodic orbit in backward time. As for the forward time, a trajectory on W^u follows the path of the bursting regime, i.e., moves leftwards along the lower, hyperpolarized branch of M_{eq}, and, provided that $z_{\mathrm{sn}} < z_{bs}$, returns to the saddle-node orbit from the left, as seen in Fig. 1(b). Thus, globally the unstable manifold W^u is homoclinic to the periodic orbit. This is the second component of the blue-sky catastrophe.

When $\alpha > \alpha_0$, i.e., the average nullcline is lifted up, the saddle-node orbit decouples into stable and unstable ones. The former corresponds to tonic spiking. When the nullcline is lowered, the saddle-node periodic orbit vanishes and gives rise to a new stable periodic orbit of a large period and amplitude, which corresponds to bursting. This orbit consists of two phases, silent (interburst) and spiking.

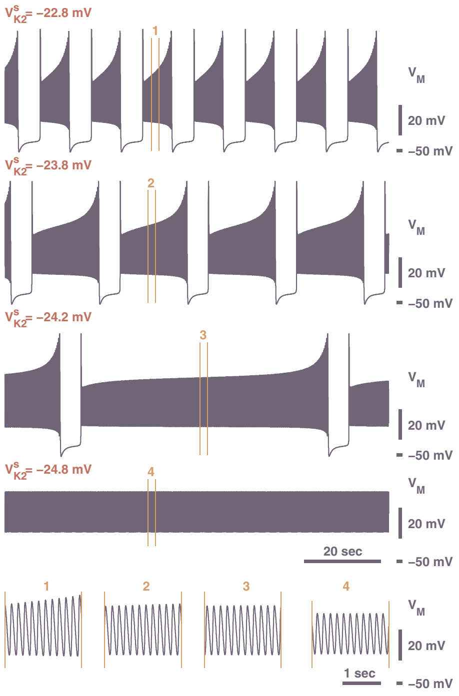

FIG. 2 (color online). Samples of oscillatory waveforms generated by the neuron model (1) for decreasing values of the bifurcation parameter V^s_{K2}. The bursting regime (the three top traces) is continuously transformed into tonic spiking (the bottom trace). The burst duration increases as V^s_{K2} approaches the blue-sky bifurcation's value ($V^s_{\mathrm{K2}} = 24.25$ mV). The bottom chart samples the spiking oscillations from the traces above.

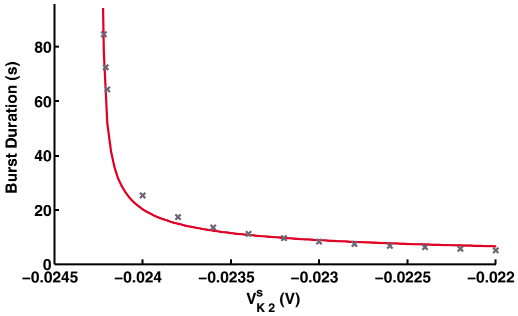

FIG. 3 (color online). Dependence of the period of bursting on the control parameter V^s_{K2}. The numerically obtained points are marked by ×'s. The curve is given by $0.31/\sqrt{|(V^s_{\mathrm{K2}} + 24.25)|}$, where 24.25 mV is the critical value of the transition.

The burst duration, the time interval that the phase point needs to pass by the phantom of the saddle node, is estimated as $1/\sqrt{\alpha - \alpha_0}$. Hence, by adjusting the deviation of α from the critical value α_0 one may control the burst duration without changing the interburst interval (see Figs. 2 and 3). Thus, a continuous transition from the bursting into tonic spiking is achieved by a single parameter variation. This transition is demonstrated in the model (1) in Fig. 2. The parameter V^s_{K2} plays the role of the control parameter α. Variations of V^s_{K2} determine the position of the average nullcline $\langle m'_{\mathrm{K2}} \rangle = 0$. As V^s_{K2} approaches the critical value 24.25 mV the duration of the bursting interval increases with no bound as predicted. The standard deviation of the period of bursting remains zero while the parameter is varied, thereby confirming that bursting is, indeed, represented by a stable periodic orbit. If one changes the parameter backwards, then the system will regain the round, stable periodic orbit corresponding to spiking. This kind of the boundary between the regimes can be called *safe* [18].

Asymptotic estimates of the dependence of temporal characteristics of bursting on the control parameter are in a good agreement with the numerically obtained data for the neuron model (Fig. 3). The period of bursting suffices for the same estimate, because the interburst interval remains almost constant. As V^s_{K2} changes from −22.20 to −24.25 mV the interburst interval decreases from 6.16 to 5.51 s, compared to the burst duration growing from 5.66 to 957 s. The spike frequency remains nearly constant around 5.5 Hz, which is a physiologically observable value. The number of spikes in a burst is proportional to the duration of the burst.

We propose a new mechanism of continuous transition between tonic spiking and bursting regimes in a model of a pharmacologically treated leech heart interneuron. This transition based on the bifurcation of the blue-sky catastrophe is generic for a broad class of neuronal models utilizing Hodgkin-Huxley formalism.

A. S. acknowledges the RFBR Grants No. 02-01-00273 and No. 01-01-00975. G. C. is supported by NIH Grant No. NS43098. We acknowledge GSU Research team and Brains & Behaviors grants. We are grateful to Yu. Kuznetsov for help on advanced features of the software package CONTENT (ftp://ftp.cwi.nl/pub/CONTENT).

---

*Electronic address: ashilnikov@gsu.edu

[1] J. Rinzel, Lect. Notes Math. **1151**, 304 (1985).
[2] J. Guckenheimer, S. Gueron, and R. M. Harris-Warrick, Philos. Trans. R. Soc. London B **341**, 345 (1993).
[3] R. Bertram, M. J. Butte , T. Kiemel, and A. Sherman, Bull. Math. Biol. **57**, 413 (1995).
[4] E. Izhikevich, J. Bifurcations Chaos **10**, 1171 (2000).
[5] D. Terman, J. Nonlinear Sci. **2**, 133 (1992).
[6] X. J. Wang, Physica (Amsterdam) **62D**, 263 (1993).
[7] P. F. Rowat and R. C. Elson, J. Comput. Neurosci. **16**, 87 112 (2004).
[8] V. N. Belykh, I. V. Belykh, M. Colding-Joregensen, and E. Mosekilde, Eur. Phys. J. E **3**, 205 (2000).
[9] C. R. Laing, B. Doiron, A. Longtin, L. Noonan, R. W. Turner, and L. Maler, J. Comput. Neurosci. **14**, 329 (2003).
[10] B. Ermentrout, Neural Comput. **8**, 979 (1996).
[11] J. Rinzel and B. Ermentrout, in *Methods in Neuronal Modeling* (The MIT Press, Cambridge, London, 1998).
[12] D. Hansel, G. Mato, and C. Meunier, Neural Comput. **7**, 307 (1995).
[13] U. Feudel, A. Neiman, X. Pei, W. Wojtenek, H. Braun, M. Huber, and F. Moss, Chaos **10**, 231 (2000).
[14] H. A. Braun, M. T. Huber, M. De Wald, K. Sshaffer, and K. Voigt, J. Bifurcations Chaos **8**, 881 (1998).
[15] A. Shilnikov, R. Calabrese, and G. Cymbalyuk (to be published).
[16] V. Lukaynov and L. Shilnikov, Sov. Math. Dokl. **19**, 1314 (1978).
[17] L. P. Shilnikov and D. V. Turaev, Comput. Math. Appl. **34**, 441 (1997).
[18] L. Shilnikov, A. Shilnikov, D. Turaev, and L. Chua, *Methods of Qualitative Theory in Nonlinear Dynamics* (World Scientific, River Edge, NJ, 1998, 2001), Vols. I–II.
[19] L. Shilnikov and D. Turaev, Am. Math. Soc. Transl., II Ser. **200**, 165 (2000).
[20] A. Shilnikov, L. Shilnikov, and D. Turaev, Moscow Math. J. (to be published).
[21] G. S. Cymbalyuk and R. L. Calabrese, Neurocomputing **38–40**, 159 (2001).
[22] G. S. Cymbalyuk, Q. Gaudry, M. A. Masino, and R. L. Calabrese, J. Neurosci. **22**, 10 580 (2002).
[23] A. Hill, J. Lu, M. Masino, O. Olsen, and R. L. Calabrese, J. Comput. Neurosci. **10**, 281 (2001).
[24] C. A. Opdyke and R. L. Calabrese, J. Comp. Physiol. **175**, 781 (1994).
[25] A. L. Hodgkin and A. F. Huxley, J. Physiol. **117**, 500 (1952).
[26] L. S. Pontryagin and L. V. Rodygin, Sov. Math. Dokl. **1**, 611 (1960).